

# Top-quark production in proton-nucleus and nucleus-nucleus collisions at LHC energies and beyond

David d'Enterria<sup>1</sup>, Krisztián Krajczár<sup>1</sup>, and Hannu Paukkunen<sup>2,3</sup>

<sup>1</sup> CERN, PH Department, 1211 Geneva, Switzerland

<sup>2</sup> Department of Physics, University of Jyväskylä, P.O. Box 35, FI-40014 University of Jyväskylä, Finland

<sup>3</sup> Helsinki Institute of Physics, P.O. Box 64, FI-00014 University of Helsinki, Finland

## Abstract

Single and pair top-quark production in proton-lead (p-Pb) and lead-lead (Pb-Pb) collisions at the CERN Large Hadron Collider (LHC) and future circular collider (FCC) energies, are studied with next-to-leading-order perturbative QCD calculations including nuclear parton distribution functions. At the LHC, the pair-production cross sections amount to  $\sigma_{t\bar{t}} = 3.4 \mu\text{b}$  in Pb-Pb at  $\sqrt{s_{\text{NN}}} = 5.5 \text{ TeV}$ , and  $\sigma_{t\bar{t}} = 60 \text{ nb}$  in p-Pb at  $\sqrt{s_{\text{NN}}} = 8.8 \text{ TeV}$ . At the FCC energies of  $\sqrt{s_{\text{NN}}} = 39$  and  $63 \text{ TeV}$ , the same cross sections are factors of 90 and 55 times larger respectively. In the leptonic final-state  $t\bar{t} \rightarrow W^+ b W^- \bar{b} \rightarrow b \bar{b} \ell \ell \nu \nu$ , after typical acceptance and efficiency cuts, one expects about 90 and 300 top-quarks per nominal LHC-year and  $4.7 \cdot 10^4$  and  $10^5$  per FCC-year in Pb-Pb and p-Pb collisions respectively. The total  $t\bar{t}$  cross sections, dominated by gluon fusion processes, are enhanced by 3–8% in nuclear compared to p-p collisions due to an overall net gluon antishadowing, although different regions of their differential distributions are depleted due to shadowing or EMC-effect corrections. The rapidity distributions of the decay leptons in  $t\bar{t}$  processes can be used to reduce the uncertainty on the Pb gluon density at high virtualities by up to 30% at the LHC (full heavy-ion programme), and by 70% per FCC-year. The cross sections for single-top production in electroweak processes are also computed, yielding about a factor of 30 smaller number of measurable top-quarks after cuts, per system and per year.

## 1 Introduction

The multi-TeV energies available at the CERN Large Hadron Collider (LHC) have opened up the possibility to measure, for the first time in heavy-ion collisions, various large-mass elementary particles. After the first observations of the  $W$  [1, 2] and  $Z$  [3, 4] bosons, as well as bottom-quark ( $b$ -jets) [5], there remains only three Standard Model (SM) elementary particles to be directly measured in nucleus-nucleus collisions: the  $\tau$  lepton, the Higgs boson, and the top quark. Whereas the  $\tau$  measurement should be straightforward, that of the Higgs boson is beyond the LHC reach as it requires much larger cross sections and/or luminosities [6], such as those reachable at the proposed future circular collider (FCC) [7] with about seven times larger center-of-mass energies than at the LHC. The study presented here shows, for the first time, that the top-quark –the heaviest elementary particle known– will be produced (singly or in pairs) in sufficiently large numbers to be observed in lead-lead (Pb-Pb) and proton-lead (p-Pb) collisions at the LHC and FCC.

Since the width of the top-quark ( $\Gamma_t \approx 2 \text{ GeV}$ ) is much larger than the parton-to-hadron transition scale given by  $\Lambda_{\text{QCD}} \approx 0.2 \text{ GeV}$ , the top-quark is the only coloured particle that decays before its hadronization. Its short lifetime,  $\tau_0 = \hbar/\Gamma_t \approx 0.1 \text{ fm}/c$ , implies that the top decays –into a  $t \rightarrow W b$  final-state with a nearly 100% branching ratio [8]– mostly<sup>1</sup> within the strongly-interacting medium, such as the quark-gluon plasma (QGP), formed in nuclear collisions. The large top-quark mass ( $m_t \approx 173 \text{ GeV}$ ) provides a hard scale for high-accuracy perturbative

<sup>1</sup>The typical transverse momentum of the produced top quark is usually smaller than its mass,  $p_T < m_t$ , and the Lorentz-boost factor is  $\gamma \approx \cosh(y_t)$ , where  $y_t$  is the  $t$ -quark rapidity. At the LHC ( $|y_t| < 3$ ) the Lorentz-dilated mean decay time is  $\tau = \gamma\tau_0 \approx 0.1 - 1 \text{ fm}/c$ , and at the FCC ( $|y_t| < 5$ ),  $\tau = \gamma\tau_0 \approx 0.1 - 7.5 \text{ fm}/c$ ; to be compared with the typical QGP formation time of  $1 \text{ fm}/c$ , and lifetime of  $10 - 20 \text{ fm}/c$ .

calculations of its quantum-chromodynamics (QCD) and electroweak production cross sections (next-to-next-to-leading-order, or NNLO, is the current theoretical state-of-the-art [9–11]). At hadron colliders, top quarks are produced either in pairs, dominantly through the strong interaction, or singly through the weak interaction. At the energies considered here, the dominant production channels, as obtained at NLO accuracy with the MCFM code [12], are: (i) gluon-gluon fusion,  $gg \rightarrow t\bar{t} + X$ , contributing by 80–95% to the total pair production (the remaining 5–20% issuing from quark-antiquark annihilation), (ii)  $t$ -channel single-top electroweak production  $qb \rightarrow q't + X$  (the  $s$ -channel process, decreasing with energy, amounts to 5–1.5% of the total single- $t$  cross section), and (iii) associated top plus  $W$ -boson,  $gb \rightarrow Wt + X$ , production (increasing with energy, it amounts to 25–50% of the  $t$ -channel process).

The theoretical motivations for a dedicated experimental measurement of the top-quark in heavy-ion collisions are varied and include, at least, the following studies:

- (i) Constraints on nuclear parton distribution functions (nPDFs). The  $t\bar{t}$  cross sections in proton-proton (p-p) collisions can be used to constrain the proton PDFs [13]. In the heavy-ion case, top-pair production probes the nuclear gluon density in an unexplored kinematic regime around Bjorken  $x \approx 2m_t/\sqrt{s_{\text{NN}}} \approx 5 \cdot 10^{-3}$ –0.05 and virtualities  $Q^2 \approx m_t^2 \approx 3 \cdot 10^4 \text{ GeV}^2$ , a region characterized by net positive, albeit small, anti-shadowing corrections. In addition, at the FCC, the  $b$ -quark nPDF (in single-top production), and even the top-quark nPDF itself, are generated dynamically by the gluons and are ingredients of the theoretical cross section calculations.
- (ii) Heavy-quark energy loss dynamics. The top quark can radiate gluons before its  $Wb$  decay which, given its very-short lifetime, occurs mostly inside the QGP. Medium-induced gluon radiation off light-quarks and gluons, leading to “jet quenching” [14], results in a factor of two reduction of jet yields in Pb-Pb compared to p-p collisions at  $\sqrt{s_{\text{NN}}} = 2.76 \text{ TeV}$  [15, 16]. Although solid theoretical expectations for heavy-quark radiation predict a reduced amount of gluonstrahlung at small angles due to the “dead cone” effect [17], the experimental data surprisingly shows the same amount of suppression for jets from light-flavours and  $b$ -quarks [5]. The relative role of elastic and radiative scatterings on the energy loss of heavy-quarks is an open issue in the field [18, 19]. The detailed study of top-quark production in heavy-ion collisions would therefore provide novel interesting insights on the mechanisms of parton energy loss. In addition, the study of boosted top-pairs (with transverse momenta above  $p_T \approx 1 \text{ TeV}$ ) traversing the QGP as a colour-singlet object for a fraction of their time, will allow one to probe the medium opacity at different space-time scales.
- (iii) Colour reconnection in the QGP. The top mass, featuring the strongest coupling to the Higgs field, is a fundamental SM parameter with far-reaching implications including the stability of the electroweak vacuum [20]. Currently, the dominant  $m_t$  systematic uncertainty is of theoretical nature and connected to the modeling of the colour connection and QCD interferences between the  $t\bar{t}$  production and decay stages, and among the hadronic decay products. Indeed, the colour-flow (through gluon exchanges and/or non-perturbative string overlaps) between the  $t$  and  $\bar{t}$  quarks, their decayed  $b$ -quarks, and the underlying event from multi-parton interactions and beam-remnants surrounding the initial hard scattering [21], results in uncertainties on the reconstructed  $m_t$  of a few hundred MeV. The amount of top quark interactions with the colour fields stretched among many partons involved in nuclear collisions will be obviously enhanced compared to more elementary systems. Thus, the reconstruction of the top-quark mass in the QGP (assuming its feasibility is not jeopardized by the large  $b$ -quark energy loss already observed in the data), or in proton-nucleus interactions, would provide interesting insights in non-perturbative QCD effects on a crucial SM parameter.

In this paper we mostly focus on nPDF constraints through top-pair production in p-Pb and Pb-Pb collisions. We also provide the expected  $p_T$  reach of top quark spectra at various energies to indicate where boosted final-states can be measured for energy loss studies. The paper is organized as follows. In Section 2 the theoretical setup used is outlined, which is then used to compute the NLO cross sections at the LHC and FCC, and associated yields expected after typical acceptance and efficiency cuts, for top-pair and single-top production, presented in Section 3. Section 4 quantifies the impact on the nuclear PDFs provided by the measurement of the rapidity distributions of the decay leptons from top-quark pairs produced at the LHC and FCC, using a Hessian PDF reweighting technique [22, 23]. The main conclusions of the work are then summarized in Section 5.

## 2 Theoretical setup

The top-pair and single-top cross sections are computed at NLO accuracy with the MCFM code [12] (version 6.7) using the central NLO set of the CT10 proton PDF [24] corrected for nuclear effects (shadowing, antishadowing and EMC) [25] through the EPS09 nPDFs (including its 30 error sets) for the Pb ion [26]. As our main purpose is to provide estimates for the feasibility of different top-quark measurements in nuclear collisions, we do not discuss here the (subleading) sensitivity of the cross sections to different sets of proton PDFs (nor associated variations of the strong coupling  $\alpha_s$ ). Also, while there are other nuclear PDF sets available [27–29], we only employ EPS09 here as it is the only nPDF set that is consistent with the dijet measurements in p-Pb collisions at the LHC [30, 31] (the data would probably agree also with the latest nPDFs by nCTEQ [32], but these sets are not available at the time of writing this article). We run the following MCFM processes:  $_{141}$  for  $t\bar{t}$  production,  $_{161, 166}$  for single-(anti)top in the  $t$ -channel,  $_{171, 176}$  in the  $s$ -channel, and  $_{181, 186}$  for associated  $tW$  production. We note that, at NLO, the theoretical processes defining  $tW$  production partially overlap with those contributing to top-quark pair production [33]. This is accounted for in our MCFM  $tW$  cross sections calculations by vetoing the additional emission of a  $b$ -jet. The code also properly accounts for the different isospin ( $u$ - and  $d$ -quark) content of the Pb nucleus, which has a small impact on the electroweak single-top processes.

All numerical results have been obtained using the latest SM parameters for particle masses, widths and couplings [8], and fixing the default renormalization and factorization scales at  $\mu = \mu_F = \mu_R = m_t$  for  $t\bar{t}$  and  $t$ -, $s$ -channel single-top, and at  $\mu = \mu_F = \mu_R = p_{T,\min;b\text{-jet}} = 50$  GeV for the  $tW$  processes. The NLO calculations used here reproduce well the cross sections experimentally measured at the LHC in p-p collisions at  $\sqrt{s} = 7, 8$  TeV for  $t\bar{t}$  [34–48],  $t$ -channel single-top [46, 49–52], and associated  $tW$  [53–55] production. Incorporation of next-to-NLO corrections [9] would increase the theoretical cross sections, by about 10%, i.e. the so-called  $K$ -factor amounts to  $K = \sigma_{\text{NNLO}}/\sigma_{\text{NLO}} \approx 1.10$ , and further improve the data-theory agreement. The computed nucleon-nucleon cross sections are scaled by the Pb mass number ( $A = 208$ ) to obtain the p-Pb cross sections, and by  $A^2 = 43\,264$  in the Pb-Pb case, as expected for hard scattering processes in nuclear collisions. The uncertainties of the theoretical cross sections are obtained by taking into account the 30 EPS09 nPDF eigenvector sets, and by independently varying the renormalization and factorization  $\mu_F$  and  $\mu_R$  scales within a factor of two. The latter scale-variation uncertainties amount to about 10% for  $t\bar{t}$  and 3–6% for single top, and have no impact on the derived nPDF constraints given that differences between proton and nuclear PDFs are obtained via ratios of (p-Pb,Pb-Pb)/(p-p) cross sections at the same colliding energy, where scale uncertainties cancel out.

## 3 Top-pair and single-top cross sections and yields

Table 1 collects the total cross sections, and associated scale and nPDF uncertainties, for top-pair and single-top production in p-Pb and Pb-Pb collisions at LHC and FCC energies, obtained as described in the previous Section. In the case of  $t\bar{t}$  and  $tW$  production, a net EPS09 gluon antishadowing in collisions with Pb ions results in an increase of the total production cross sections by about 2–8% compared to those ( $A$ -scaled) obtained for p-p collisions using the proton CT10 PDF. For  $t$ - and  $s$ -channel single-top cross sections, the overall nuclear modifications are quite insignificant,  $\pm 2\%$  depending on the energy. Figure 1 shows the total top-pair and single-top cross sections as a function of collision energy for p-p, p-Pb and Pb-Pb collisions in the range of c.m. energies in the nucleon-nucleon system of  $\sqrt{s_{\text{NN}}} \approx 1\text{--}100$  TeV. The single-top curves are obtained adding the  $t$ -, $s$ -channel and  $tW$  cross sections listed in Table 1. In general, top-quark pair production is a factor of two (four) larger than the sum of single top processes at the LHC (FCC). The nominal LHC and FCC energies for p-Pb and Pb-Pb collisions are indicated by dashed boxes in the plot. Going from LHC to FCC, the total cross sections increase by significant factors,  $\times(55\text{--}90)$  for  $t\bar{t}$  and  $\times(30\text{--}40)$  for single-top.

The impact of nuclear PDF modifications on the yields for a given hard process is usually quantified through the nuclear modification factor  $R_{\text{AA}}$  given by the ratio of cross sections in nuclear over proton-proton collisions scaled by  $A$  or  $A^2$ . The theoretical  $R_{\text{AA}}(y_{t,\bar{t}})$  factors as a function of the rapidity of the produced top and antitop quarks are shown in Fig. 2 for  $t\bar{t}$  at LHC (top panels) and FCC (bottom panels) energies. The central curves indicate the result obtained with the central EPS09 set and the grey bands show the corresponding nPDF uncertainties. In general,

Table 1: Inclusive cross sections for top-pair and single-top ( $t$ -channel,  $s$ -channel, and  $tW$ ) production in Pb-Pb and p-Pb collisions at LHC and FCC energies, obtained at NLO accuracy with MCFM. The first uncertainty is due to theoretical scale variations and the second one to the EPS09 PDF errors.

System / Process: (MCFM process)	top pairs ( $t\bar{t}$ ) (141)	single-top ( $t$ -channel) (161, 166)	single-top ( $s$ -channel) (171, 176)	single-top ( $tW$ ) (181, 186)
Pb-Pb $\sqrt{s_{NN}} = 5.5$ TeV	$3.40 \pm 0.42 \pm 0.24 \mu\text{b}$	$1.61 \pm 0.05 \pm 0.06 \mu\text{b}$	$110 \pm 4 \pm 2 \text{ nb}$	$313 \pm 13 \pm 28 \text{ nb}$
p-Pb $\sqrt{s_{NN}} = 8.8$ TeV	$58.8 \pm 7.1 \pm 1.8 \text{ nb}$	$21.1 \pm 0.63 \pm 0.42 \text{ nb}$	$1.09 \pm 0.03 \pm 0.01 \text{ nb}$	$5.26 \pm 0.21 \pm 0.16 \text{ nb}$
Pb-Pb $\sqrt{s_{NN}} = 39$ TeV	$302 \pm 33 \pm 9 \mu\text{b}$	$54.6 \pm 1.6 \pm 1.6 \mu\text{b}$	$1.31 \pm 0.05 \pm 0.07 \mu\text{b}$	$24.2 \pm 1.6 \pm 0.9 \mu\text{b}$
p-Pb $\sqrt{s_{NN}} = 63$ TeV	$3.20 \pm 0.35 \pm 0.03 \mu\text{b}$	$518 \pm 16 \pm 10 \text{ nb}$	$10.9 \pm 0.5 \pm 0.3 \text{ nb}$	$246 \pm 24 \pm 5 \text{ nb}$

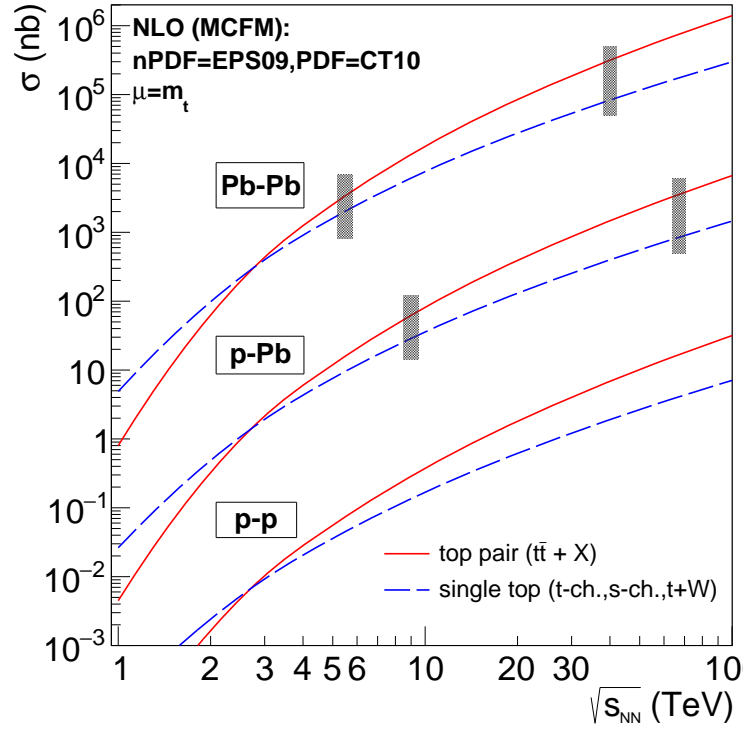


Figure 1: Total cross sections for top pair and single-top (sum of  $t$ -,  $s$ -channels plus  $tW$  processes) production in Pb-Pb p-Pb and p-p collisions as a function of c.m. energy. The dashed boxes indicate the nominal nucleon-nucleon c.m. energies,  $\sqrt{s_{NN}} = 5.5, 8.8, 39, 63$  TeV, of the heavy-ion runs at the LHC and FCC.

the  $R_{AA}(y_{t,\bar{t}})$  distributions reveal very similar trends for  $t\bar{t}$  and single-top (not shown here) processes, although the  $t$ -channel and  $s$ -channel processes have a factor of two smaller uncertainties, as expected, given that single-top production is dominated by quark-induced processes whose densities in the nucleus are better known than the gluon ones which produce most of the top-pairs. At the LHC, for both (single and pair) production mechanisms, the nPDF effects increase the average top-quark distributions at central rapidities by about 10% (antishadowing) while they deplete them by 20% at backward rapidities (also in the forward direction in Pb-Pb) due to the so-called EMC effect at large- $x$  [25] (see also Fig. 4 later). At the FCC, the higher collision energies as well as the larger kinematical coverage assumed for the detectors at this future facility give access to smaller momentum fractions  $x$  where EPS09 predicts moderate shadowing even at high virtualities  $Q \sim m_t$ . This leads to additional suppression at forward rapidities (and also in the backward direction in Pb-Pb).

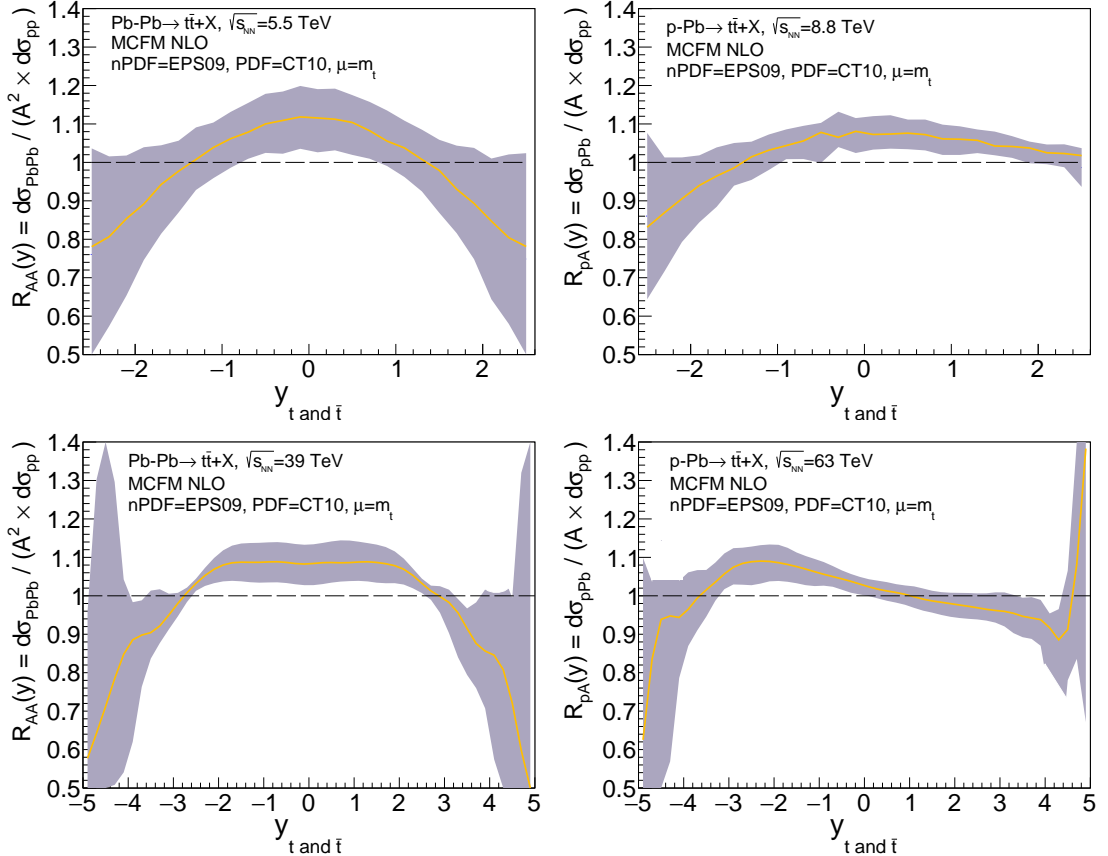


Figure 2: Theoretical nuclear modification factor as a function of the (anti)top rapidity in  $t\bar{t}$  production in Pb-Pb (left panels) and p-Pb (right panels) at  $\sqrt{s_{NN}} = 5.5, 8.8$  TeV (LHC, top panels) and 39, 63 TeV (FCC, bottom panels), computed at NLO accuracy with MCFM. The central curve indicates the result obtained with central EPS09 parametrization and the grey band the corresponding nPDF uncertainty.

The cross sections listed in Table 1 and plotted in Fig. 1 are total inclusive ones and do not include the  $t \rightarrow W b$  decays, nor any experimental acceptance/analysis requirements on the final-state particles. The determination of the expected yields at the LHC and FCC requires accounting for top and  $W$ -boson decays plus acceptance and reconstruction efficiency losses. The  $W$  leptonic branching fractions,  $W \rightarrow \ell^\pm \nu_\ell$  (with  $\ell = e, \mu, \tau$ ), amount to 1/9 for each lepton flavour, the other 2/3 being due to  $W$  dijet (quark-antiquark) decays. In this work we will only consider leptonic  $W$  decays characterized by a final-state with an isolated electron or muon plus missing transverse energy ( $E_T^{\text{miss}}$ ) from the neutrino, because the  $W$  dijet-decays are much more difficult to reconstruct in the large background of heavy-ion collisions, and also potentially subject to parton energy loss effects (although they could be certainly tried in the “cleaner” p-Pb environment). For the top-pairs measurement,  $t\bar{t} \rightarrow W^+ b W^- \bar{b} \rightarrow b \bar{b} \ell \ell \nu \nu$ , the combination of electron and muon decays for both  $W$ -bosons ( $ee, \mu\mu, e\mu, \mu e$ ) reduces the total cross sections

by a factor<sup>2</sup> of  $\mathcal{B}_{\ell\ell} = 4/9^2 \approx 1/20$ . For the single-top case, we will only consider the yields for associated  $tW$  production which shares a characteristic final-state signature,  $tW \rightarrow WbW \rightarrow b\ell\ell\nu\nu$ , very similar to that of top-pair production. Indeed, the experimental observation of  $t$ -channel (let alone the much more suppressed  $s$ -channel) single-top, with one less charged lepton and neutrino, is much more challenging on top of the expected large  $W, Z$ +jets background (in Pb-Pb, at least, although it should be feasible in p-Pb collisions).

In order to compute the expected number of top-quarks measurable at the LHC and FCC, we include in the MCFM generator-level calculations the typical analysis and fiducial requirements for  $b$ -jets, charged leptons, and missing transverse energy from the unidentified neutrinos, used in similar p-p measurements at the LHC [35, 38, 54]. Although some of these p-p experimental requirements may seem optimistic for the more complex environment encountered in heavy-ion collisions, they are validated by future experimental projections of the CMS collaboration [56]. In the case of FCC, we extend the pseudorapidity coverage for charged-lepton tracking and  $b$ -jet secondary vertexing from the LHC range of  $|\eta| = 2.5$ , to  $|\eta| = 5$ . The details of all selection criteria are given in Table 2. We reconstruct the  $b$ -jets with the anti- $k_T$  jet clustering algorithm [57] with distance parameter  $R = 0.5$ , and we require the high- $p_T$  charged lepton to be separated from the closest  $b$ -jet within an  $(\eta, \phi)$  isolation radius of  $R_{\text{isol}} = 0.3$ .

Table 2: List of analysis cuts on single  $p_T$  and  $\eta$  for  $b$ -jets and isolated leptons  $\ell = e^\pm, \mu^\pm$ , and on the neutrinos  $\cancel{E}_T$ , typically employed in top-pair ( $t\bar{t} \rightarrow b\bar{b}\ell\ell\nu\nu$ ) [35, 38] and single-top plus  $W$ -boson ( $tW \rightarrow b\ell\ell\nu\nu$ ) [54] measurements in fully-leptonic final-states in p-p collisions at the LHC, applied in our generator-level studies.

Analysis cuts
$b$ -jets (anti- $k_T$ algorithm with $R = 0.5$ ): $p_T > 30$ GeV; $ \eta  < 2.5$ (LHC), 5 (FCC)
charged leptons $\ell$ ( $R_{\text{isol}} = 0.3$ ): $p_T > 20$ GeV; $ \eta  < 2.5$ (LHC), 5 (FCC)
neutrinos: $\cancel{E}_T > 40$ GeV

The combination of all analysis cuts listed in Table 2 results in total acceptances of order  $\mathcal{A}_{t\bar{t}} \approx \mathcal{A}_{tW} \approx 40\%$  (50%) for  $t\bar{t}$  and  $tW$  measurements at the LHC (FCC). In addition, one has to account for experimental  $b$ -jet tagging efficiencies, which we conservatively take of the order of 50% as determined in Pb-Pb collisions at  $\sqrt{s} = 2.76$  TeV [5]. For single-top, this results in an extra  $\varepsilon_{tW} \approx 0.5$  reduction of the measured yields. In the  $t\bar{t}$  case, in order to tag the event as such, one usually only requires a single  $b$ -jet (out of the two produced) to be identified, and thus the associated efficiency is larger:  $\varepsilon_{t\bar{t}} \approx 1 - (1 - 0.5)^2 = 0.75$ . The combination of acceptance, analysis requirements, and efficiency losses results in an overall efficiency factor of  $\mathcal{A}_{t\bar{t}} \times \varepsilon_{t\bar{t}} \approx 30\%$  (40%) for the final  $t\bar{t}$  yields<sup>3</sup> at the LHC (FCC). The same factor for  $tW$  production is  $\mathcal{A}_{tW} \times \varepsilon_{tW} \approx 20\%$  (25%) at the LHC (FCC). Possible backgrounds, mostly from  $W, Z$ +jets,  $WZ$ , and  $ZZ$  production sharing similar final-state signatures as both top-quark production processes, can be minimized by applying dedicated jet-veto requirements and/or extra criteria on the invariant masses of the two high- $p_T$  leptons, e.g. away from the  $Z$  boson peak ( $|m_Z - m_{\ell\ell}| > 15$  GeV). We do not directly compute the impact of such backgrounds here as the applied analysis cuts already reduce them to a manageable level according to the existing p-p measurements. In particular, the application of  $m_{\ell\ell}$  cuts would reduce the visible yields by an extra 10% which is, however, compensated by the fact that our NLO calculations need to be scaled by about the same amount to match the current p-p data (and NNLO predictions). We note also that, despite the larger hadronic backgrounds in nuclear collisions, the instantaneous luminosities in the heavy-ion operation mode at the LHC (and FCC) result in a very small event pileup, at variance with the p-p case, and make the top-quark measurements accessible without the complications from overlapping nuclear collisions occurring simultaneously in the same bunch crossing.

The expected total number of top-quarks (adding the  $t$  and  $\bar{t}$  values) produced in Pb-Pb and p-Pb in one year at the nominal luminosities for each colliding system, obtained via  $\mathcal{N} = \sigma \cdot \mathcal{B}_{\ell\ell} \cdot \mathcal{L}_{\text{int}} \cdot \mathcal{A} \cdot \varepsilon$ , are listed in Table 3. The

<sup>2</sup>Including also  $e^\pm$  and  $\mu^\pm$  from leptonic tau-decays in the  $t\bar{t} \rightarrow e\tau, \mu\tau, \tau\tau + \cancel{E}_T$  final-states would decrease the corresponding branching ratio only to  $\mathcal{B}_{\ell\ell} \approx 1/16$ .

<sup>3</sup>We note that, in the Pb-Pb case, parton energy loss effects which can bring the  $b$ -jet below the  $p_T$  threshold criterion ( $p_T > 30$  GeV) and result in an additional inefficiency to tag the  $t\bar{t}$  event, are unlikely to affect both  $b$ -jets at the same time. Indeed, for simple geometrical reasons if one top-quark is produced and decays through the denser region, the other one emitted back-to-back will go through a thinner medium layer and its associated  $b$ -jet will be tagged with our considered probability.

number of visible single tops in  $tW$  processes is smaller by a factor of  $\sim 30$  compared to those from  $t\bar{t}$  production, due to a combination of causes: lower cross sections, smaller reconstruction efficiencies, and only one top-quark per event. At the LHC, we expect about 100 and 300 top-quarks measurable in the fully leptonic decays from  $t\bar{t}$ -pairs and  $tW$  processes in Pb-Pb and p-Pb respectively. At the end of the LHC heavy-ion programme, with  $\mathcal{L}_{\text{int}} \approx 10 \text{ nb}^{-1}$  ( $1 \text{ pb}^{-1}$ ) integrated in Pb-Pb (p-Pb), about 2.5 thousand (fully-leptonic) (anti)top-quarks should have been measured individually by the CMS and ATLAS experiments. The corresponding visible yields at the FCC are about 300 times larger, reaching  $5 \times 10^4$  and  $10^5$  top-quarks per year in Pb-Pb and p-Pb collisions respectively.

Table 3: Expected number of top+antitop quarks per run, after typical acceptance and efficiency losses, for top-pair and  $tW$  single-top measurements in fully-leptonic final-states in p-Pb and Pb-Pb collisions at LHC and FCC energies for the nominal per-year luminosities quoted.

System	$\sqrt{s}$	$\mathcal{L}_{\text{int}}$	Number of top+antitop quarks $t\bar{t} \rightarrow b\bar{b}\ell\ell\nu\nu$	Number of top+antitop quarks $tW \rightarrow b\ell\ell\nu\nu$
Pb-Pb	5.5 TeV	$1 \text{ nb}^{-1}$	90	3
p-Pb	8.8 TeV	$0.2 \text{ pb}^{-1}$	300	10
Pb-Pb	39. TeV	$5 \text{ nb}^{-1}$	47 000	1 300
p-Pb	63. TeV	$1 \text{ pb}^{-1}$	100 000	2 600

In order to provide an idea of the top-quark  $p_T$  reach accessible in the different measurements listed in Table 3, we have also computed the expected  $t, \bar{t}$  transverse-momentum distributions in Pb-Pb and p-Pb collisions, after all acceptance and efficiency criteria applied (Fig. 3). The maximum top-quark  $p_T$  experimentally measurable per LHC (FCC) year will be around  $p_T \sim 300$  (1500) GeV for Pb-Pb and  $p_T \sim 500$  (1800) GeV for p-Pb. Given the limited LHC top-quark statistics, the study of boosted-tops will be only accessible at the future circular collider.

## 4 Constraints on nuclear PDFs from $t\bar{t}$ production

As aforementioned, 80–95% of the total pair production at LHC–FCC comes from gluon-gluon fusion processes and, thus,  $t\bar{t}$  cross sections can be used to constrain the relatively badly-known gluon densities in the Pb nucleus. In this section we quantify the impact that top-quark measurements at the LHC and FCC would have on better constraining the nuclear PDFs through the so-called Hessian PDF reweighting technique [22, 23]. Such PDF reweighting procedure is based on the fact the error sets  $\{f\}_k^\pm$  defined in Hessian PDF-fits correspond to a certain increment  $\Delta\chi^2$  ( $\Delta\chi^2 = 50$  for EPS09) of the global “goodness-of-fit”  $\chi^2$  function whose minimum  $\chi_0^2$  is achieved with the central set  $\{f\}_0$ . The error sets thereby constitute a parametrization of the original  $\chi^2$  function which can be taken advantage of in order to determine the associated PDF uncertainty after adding new experimental datasets. More precisely, the Hessian method [58] for determining the PDF errors writes the response of the original  $\chi^2$  function to fit-parameter variations  $\delta a_i$  as

$$\chi^2\{a\} - \chi_0^2 \approx \sum_{i,j} \delta a_i H_{ij} \delta a_j = \sum_k z_k^2, \quad (1)$$

where the Hessian matrix  $H_{ij} = (1/2)\partial^2\chi^2/(\partial a_i\partial a_j)$  is diagonalized in the last step. The PDF error sets  $\{f\}_k^\pm$  are then defined by  $z_i(\{f\}_k^\pm) = \pm\sqrt{\Delta\chi^2}\delta_{ik}$ . The impact of including new experimental data can now be computed by considering a function

$$\chi_{\text{new}}^2 \equiv \sum_k z_k^2 + \sum_{i,j} [T_i(z) - D_i] C_{ij}^{-1} [T_j(z) - D_j], \quad (2)$$

where  $D_i$  denote the  $i$ th new data-point and  $C$  is the covariance matrix that encodes the experimental uncertainties. The corresponding theoretical values are denoted by  $T_i$  and they depend on the PDFs. To first approximation, the  $z$

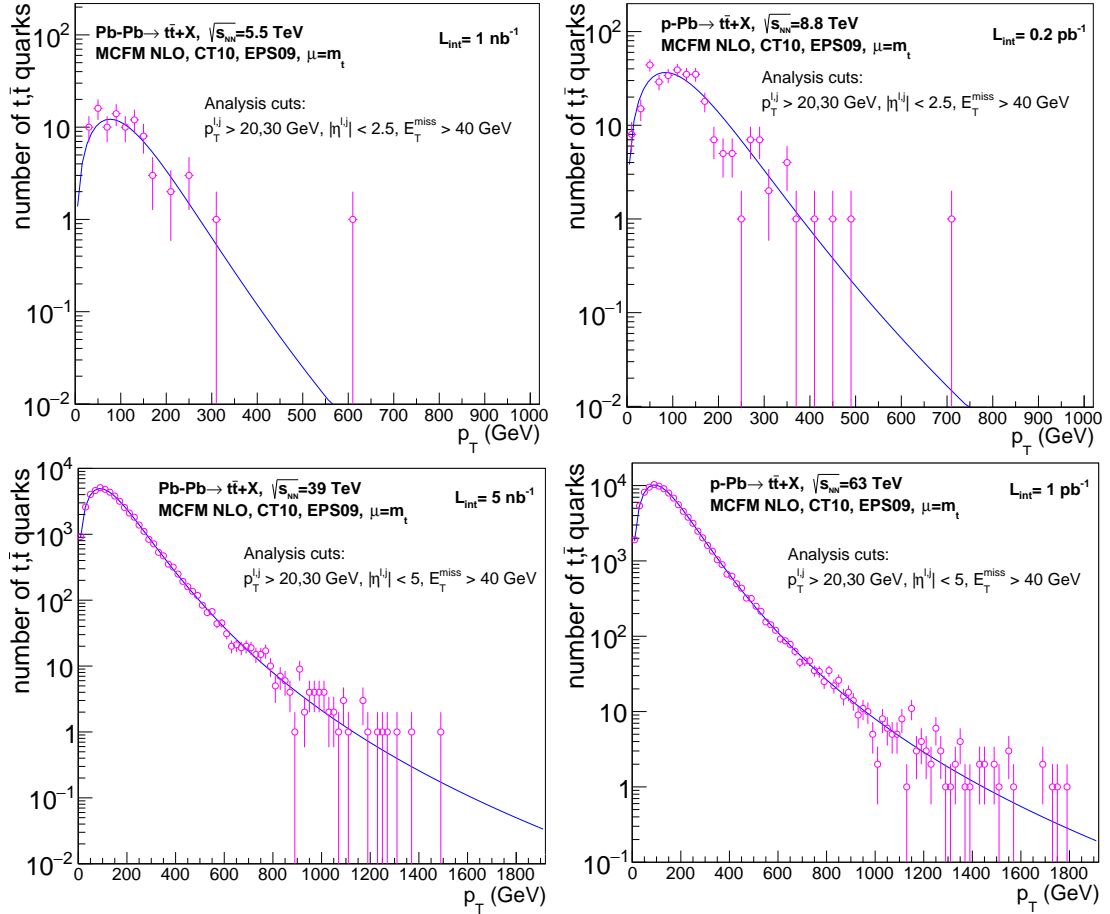


Figure 3: Expected top-quark  $p_T$  distributions in Pb-Pb (left panels) and p-Pb (right panels) in the fully-leptonic decay modes at  $\sqrt{s_{NN}} = 5.5, 8.8$  TeV (LHC, top panels) and 39, 63 TeV (FCC, bottom panels) after acceptance and efficiency cuts. The curves are a fit to the underlying MCFM distribution. The markers indicate pseudodata corresponding to the luminosities listed in Table 3.

dependence of each  $T_i$  is given by

$$T_i(z) \approx T_i(0) + \sum_k \frac{T_i(z_k^+) - T_i(z_k^-)}{2} w_k, \quad (3)$$

where  $w_k \equiv z_k / \sqrt{\Delta\chi^2}$ ,  $T_i(0)$  is the theory value computed with the central set  $\{f\}_0$ , and  $T_i(z_k^\pm)$  is the theory value evaluated with the error set  $\{f\}_k^\pm$ . Inserting Eq. (3) into Eq. (2) and requiring  $\partial\chi_{\text{new}}^2/\partial w_k = 0$  for all  $k$ , one finds the condition  $w_k^{\text{min}} = -\sum_i B_{ki}^{-1} a_i$  for the minimum of  $\chi_{\text{new}}^2$ , where  $B_{kn} = \sum_{i,j} D_{ik} C_{ij}^{-1} D_{jn} + \Delta\chi^2 \delta_{kn}$ ,  $a_k = \sum_{i,j} D_{ik} C_{ij}^{-1} [T_j(0) - D_j]$ , and  $D_{ik} = (T_i(z_k^+) - T_i(z_k^-))/2$ . The new theory values  $T_i^{\text{new}}$  are obtained directly from Eq. (3) with  $w_k = w_k^{\text{min}}$ , and the corresponding new central set of PDFs  $\{f^{\text{new}}\}_0$  by replacing  $T_i$  with the PDFs,  $T_i \rightarrow f^{\text{new}}(x, Q^2)$ . To find the new PDF error sets  $\{f^{\text{new}}\}_k^\pm$ , we rewrite Eq. (2) as

$$\chi_{\text{new}}^2 - \chi_{\text{new}}^2|_{\mathbf{w}=\mathbf{w}^{\text{min}}} = \sum_{i,j} \delta w_i B_{ij} \delta w_j = \sum_k v_k^2, \quad (4)$$

where  $\delta w_i = w_i - w_i^{\text{min}}$ , and in the last step the matrix  $B$  is being diagonalized. The new PDF error sets  $\{f^{\text{new}}\}_k^\pm$  can be then defined exactly as earlier by  $v_i(\{f^{\text{new}}\}_k^\pm) = \pm\sqrt{\Delta\chi^2} \delta_{ik}$ . The procedure sketched above was proven in Ref. [23] to be consistent with the Bayesian reweighting method introduced originally in Ref. [59] and further confirmed more recently in Ref. [60].

To mimic a realistic experimental situation, we generate sets of pseudodata for nuclear-modification factors  $R_{\text{pPb}}$  and  $R_{\text{PbPb}}$  –i.e. for the ratios of cross sections obtained with EPS09 nPDFs over those obtained with the CT10 proton PDFs– corresponding to the LHC and FCC scenarios discussed in the previous Section. As noted earlier, the total  $t\bar{t}$  production cross section is expected to undergo only a mild increase due to nuclear effects in the nPDFs, and it may be challenging to resolve such an effect from overall normalization uncertainties. Thus, the total  $t\bar{t}$  cross sections are not expected to have as large impact as they have on the absolute free proton PDFs [13]. In order to get better constraints on the nPDFs differential cross sections are thus needed. For this purpose, we use the distributions of leptonic top-decay products, which are unaffected by final-state interactions in the strongly-interacting matter produced in nuclear collisions. Here, we concentrate on the measurement of  $t\bar{t}$  pairs via the  $t\bar{t} \rightarrow b\bar{b} + \ell^+\ell^- + \nu\bar{\nu}$  decay channel, binned in the charged lepton rapidity  $dN_\ell/dy_\ell$  with  $\ell = e, \mu$ . The baseline for the pseudodata is taken from the nuclear modification factors computed with the central set of EPS09 in the previous Section. The expected number of events  $N(\Delta y_i)$  in each rapidity bin  $\Delta y_i$  are computed by

$$N(\Delta y_i) = N_{\text{total}} \times \frac{\sigma(y_i \in \Delta y)}{\sigma_{\text{total}}}, \quad (5)$$

where  $N_{\text{total}}$  is the total number of events expected after acceptance and efficiency losses for each system<sup>4</sup> listed in Table 3,  $\sigma(y_i \in \Delta y)$  is the cross section within rapidity bin  $\Delta y_i$ , and  $\sigma_{\text{total}}$  is the total cross section within the acceptance. The statistical uncertainty is then taken to be  $\delta_i^{\text{stat}} = T_i^{\text{EPS09}} \sqrt{1/N(\Delta y_i)}$  to which we add in quadrature a constant  $\pm 5\%$  systematic error ( $\delta_i^{\text{systr}} = 0.05 \times T_i^{\text{EPS09}}$ ), such that the total uncorrelated error is  $\delta_i^{\text{uncorr}} = \sqrt{(\delta_i^{\text{stat}})^2 + (\delta_i^{\text{systr}})^2}$ . The overall normalization error is taken to be 5% ( $\delta_i^{\text{norm}} = 0.05 \times T_i^{\text{EPS09}}$ ). Systematic uncertainties of this order (in fact, somewhat better) have been reached in the corresponding p-p measurements at the LHC [38, 39]. Each pseudodata point  $D_i$  is then computed from the baseline values  $T_i^{\text{EPS09}}$  and from the estimated uncorrelated and normalization errors by  $D_i = (T_i^{\text{EPS09}} + \delta_i^{\text{uncorr}} r_i + \delta_i^{\text{norm}} r^{\text{norm}})$ , where  $r_i$  and  $r^{\text{norm}}$  are random numbers from a Gaussian distribution of variance one centered around zero. The elements of the covariance matrix  $C$  are computed as  $C_{ij} = [\delta_i^{\text{uncorr}} \delta_j^{\text{uncorr}} \delta_{ij} + \delta_i^{\text{norm}} \delta_j^{\text{norm}}]$  [61].

In the original EPS09 analysis [26], the inclusive pion data measured at RHIC [62] was given an additional weight factor of 20 in the  $\chi^2$ -function in order to enhance the constraints on the badly known gluon densities from nuclear deep-inelastic and fixed-target Drell-Yan data alone. As both the pion data and the top quark production considered here, are mostly sensitive to nuclear gluon PDFs, we rescale the covariance matrix equally by  $C \rightarrow C/20$  when performing the reweighting. This compensates for the large weight given for the RHIC pion data and should

<sup>4</sup>For the LHC, we consider the total luminosity to be accumulated during the full heavy-ion programme, which is a factor of 10 (5) higher than the nominal per-year luminosities quoted for Pb-Pb (p-Pb).

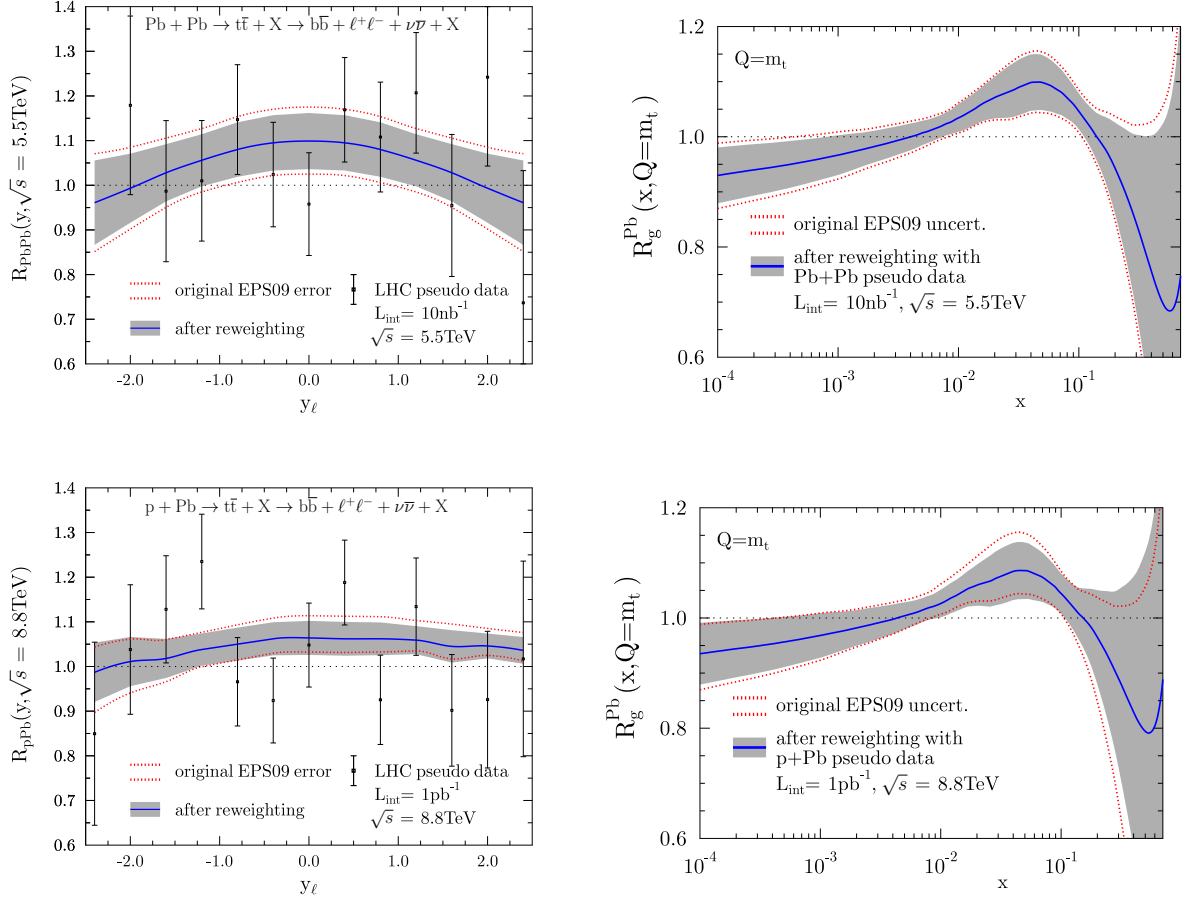


Figure 4: Impact on the nuclear glue of  $t\bar{t}$  (pseudo) data for the full LHC heavy-ion programme. Left: Nuclear modification factor for  $t\bar{t}$  decay-leptons as a function of rapidity,  $R_{\text{PbPb}}(y_\ell)$ , obtained for Pb-Pb at  $\sqrt{s_{\text{NN}}} = 5.5$  TeV (top) and p-Pb at  $\sqrt{s_{\text{NN}}} = 8.8$  TeV (bottom) compared to predictions computed with EPS09: current nPDF set (region enclosed by the red dotted lines) and after pseudodata-reweighting (blue curve plus grey band). Right: Ratio of nuclear-over-proton gluon densities,  $R_g^{\text{Pb}}(x, Q=m_t)$  evaluated at  $Q^2 = m_t$ , for the original EPS09 (band enclosed by red dotted lines) and for the reweighted EPS09 (blue curve with grey band) for Pb-Pb (top) and p-Pb (bottom).

lead to a more realistic estimate of the impact that the top-quark measurements would have if directly included into the EPS09 fit. After finding the new theory values  $T_i^{\text{new}}$  through the reweighting procedure, the optimum overall shift (originating from the allowed uncertainty in normalization) is found by solving the multiplicative factor  $f$  from the  $\chi^2$  contribution of the new data (see e.g. Ref. [61]):

$$\sum_{i,j} [T_i^{\text{new}} - D_i] C_{ij}^{-1} [T_j^{\text{new}} - D_j] = \min \left\{ \sum_i \left[ \frac{T_i^{\text{new}} - D_i - f \delta_i^{\text{norm}}}{\delta_i^{\text{uncorr}}} \right]^2 + f^2 \right\}. \quad (6)$$

In the results presented below, the resulting shift  $f \delta_i^{\text{norm}}$  has been applied on the data points.

The results of the nPDF reweighting procedure are presented first for LHC energies in Figure 4 for Pb-Pb (top) and p-Pb (bottom) collisions. The nuclear modifications for the decay leptons are somewhat less pronounced in comparison to the top distributions themselves (Fig. 2) due to the smoothing brought about by the additional phase-space integrations related to the top decay products. The estimated statistical errors are generally of the order of 10% and are foreseen to dominate over the predicted systematic uncertainties. In both cases the pseudodata are found to have only a moderate impact on the EPS09 gluon density. This is predominantly due to the rather low foreseen statistics plus also due to the limited rapidity interval covered, which makes especially  $R_{\text{pPb}}(y_\ell)$  somewhat flat

within the acceptance. Consequently, even the overall normalization alone can mimic the effects of nuclear PDFs thereby reducing the obtainable constraints. The new error bands in Figs. 4 are both around 10% narrower than the original EPS09 ones. Combining the p-Pb and Pb-Pb measurements and assuming independent data samples available from both the CMS and ATLAS collaborations, the total impact of  $t\bar{t}$  production on the large- and mid- $x$  nuclear gluons could reach 30% (with the full LHC luminosity). Such a modest improvement will most likely be overpowered by the constraints offered by the inclusive jet and dijet data from the LHC p-Pb run(s) [31].

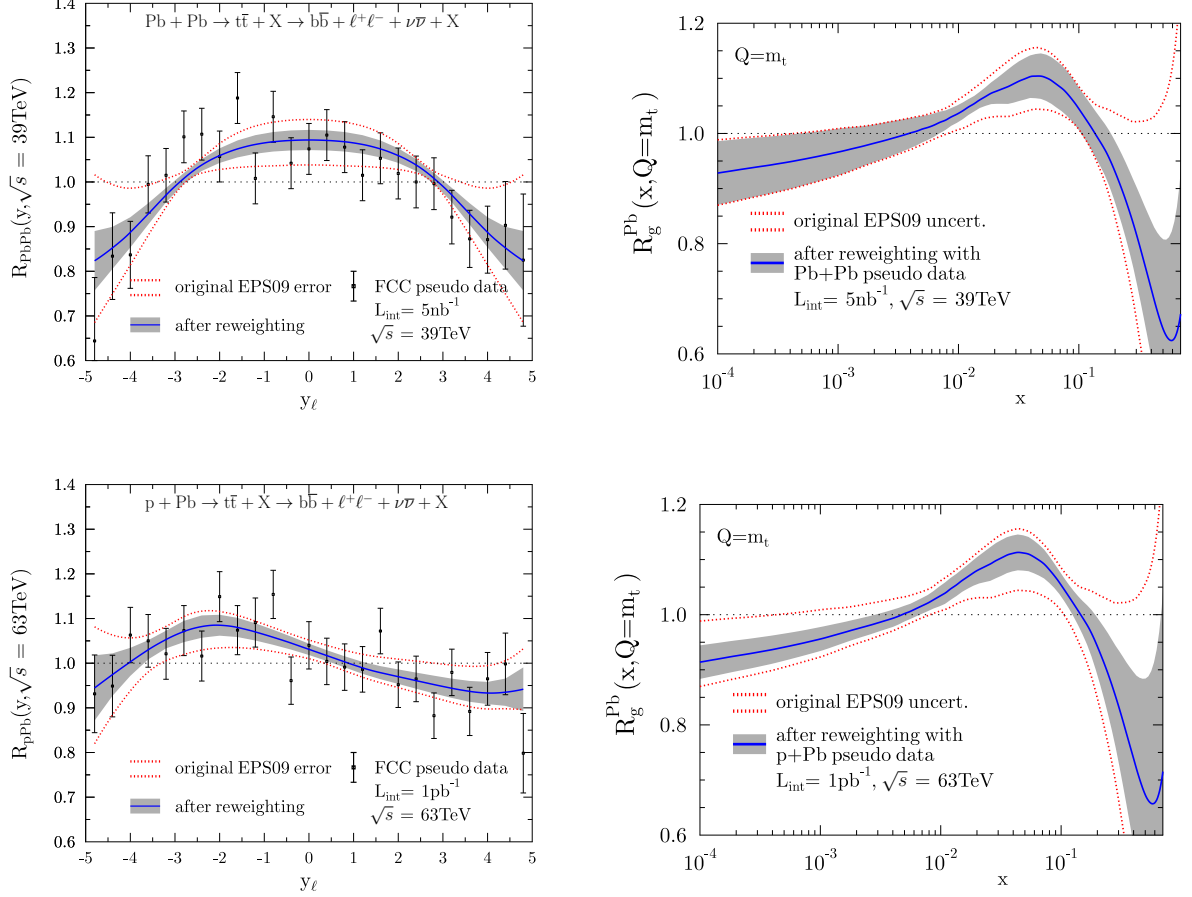


Figure 5: As Figure 4 but for the case of Pb-Pb (top) and p-Pb (bottom) per FCC-year pseudodata.

The results of repeating the reweighting procedure with the FCC pseudodata are shown in Fig. 5 for Pb-Pb (top) and p-Pb (bottom) collisions respectively. Although the foreseen FCC per-year integrated luminosities are similar to those expected for the *full* LHC heavy-ion programme, the production cross sections being a factor  $\times(55\text{--}90)$  above the LHC expectations (Table 3) significantly increase the expected top-quark yields thereby reducing the statistical uncertainties. Indeed, in our FCC scenario the systematic uncertainties dominate. The reduced uncertainties as well as the wider kinematic reach at the FCC make the impact of these pseudodata on EPS09 clearly larger than that expected at the LHC. The constraints also reach lower values of  $x$ . The addition of the nuclear  $t\bar{t}$  results shown in Fig. 5 allows one to decrease the gluon density uncertainty by up to 50% in some regions. Combination of p-Pb and Pb-Pb data, plus assumption of two independent experiments measuring the spectra, would result in an overall reduction of up to 70% with just one year of integrated luminosity.

## 5 Conclusions

The study presented here has shown, for the first time, that top quarks produced in pairs via (mostly) gluon-gluon fusion or singly in electroweak processes, are clearly observable in p-Pb and Pb-Pb collisions at the energies of the CERN LHC and future circular collider (FCC). The corresponding cross sections have been computed at NLO accuracy with the MCFM code including the CT10 free proton PDFs and nuclear modifications parametrized with the EPS09 nPDF. At the LHC, the pair-production cross sections are  $\sigma_{t\bar{t}} = 3.4 \mu\text{b}$  for Pb-Pb at  $\sqrt{s_{\text{NN}}} = 5.5$ , and  $\sigma_{t\bar{t}} = 50 \text{ nb}$  for p-Pb at  $\sqrt{s_{\text{NN}}} = 8.8 \text{ TeV}$ . At the FCC energies of  $\sqrt{s_{\text{NN}}} = 39, 63 \text{ TeV}$ , the same cross sections are factors of 90 and 55 times larger respectively. The total  $t\bar{t}$  cross sections are enhanced by 3–8% in nuclear compared to p-p collisions at the same c.m. energies, due to an overall net gluon antishadowing, although different regions of the top-quark differential distributions are depleted due to shadowing and EMC-effect corrections. The total cross sections for single-top, including the sum of  $t$ - and  $s$ -channels plus associated  $tW$  processes, are a factor of two (four) smaller than that for top-pair production at the LHC (FCC) and feature minimal nuclear modifications ( $\pm 2\%$  depending on the energy).

After applying typical acceptance and efficiency cuts in the leptonic final-state,  $t\bar{t} \rightarrow W^+bW^-\bar{b} \rightarrow b\bar{b}\ell\ell\nu\nu$ , one expects about 100 and 300 (anti)top-quarks per LHC-year and  $5 \times 10^4$  and  $10^5$  per FCC-year at the nominal luminosities in Pb-Pb and p-Pb collisions respectively. At the end of the LHC heavy-ion programme, with  $\mathcal{L}_{\text{int}} \approx 10 \text{ nb}^{-1}, 1 \text{ pb}^{-1}$  integrated Pb-Pb and p-Pb luminosities, about 2.5 thousand (fully-leptonic)  $t, \bar{t}$ -quarks should have been measured individually by the CMS and ATLAS experiments. The number of visible single-top quarks produced in association with a W boson, in the similar  $tW \rightarrow WbW \rightarrow b\ell\ell\nu\nu$  final state, is lower by a factor of about 30 compared to  $t\bar{t}$  production, due to the combination of lower cross sections, smaller reconstruction efficiencies, and only one top-quark per event.

The proposed top-quark measurements at the LHC and FCC would not only constitute the first observation in nuclear collisions of the heaviest-known elementary particle, but would open up interesting novel physics opportunities such as constraints of nuclear parton densities in an unexplored kinematic range, studies of the dynamics of heavy-quark energy loss in the QGP, and colour-reconnection effects on the top-quark mass. We have, in particular, quantified the impact on the nuclear PDFs of the rapidity-differential distributions of the decay leptons from top-quark pairs, through the Hessian reweighting technique, finding that the data can be used to reduce the uncertainty on the Pb gluon density at high virtualities by 30% using the full LHC heavy-ion programme, and by about 70% with just one FCC-year.

## Acknowledgments

We are grateful to Carlos Salgado for early discussions on this work, and to Martijn Mulders for feedback on the manuscript. K.K. acknowledges partial financial support from the Hungarian Scientific Research Fund (K 109703).

## References

- [1] S. Chatrchyan *et al.* [CMS Collaboration], Phys. Lett. B **715** (2012) 66 [arXiv:1205.6334 [nucl-ex]].
- [2] G. Aad *et al.* [ATLAS Collaboration], arXiv:1408.4674 [hep-ex].
- [3] S. Chatrchyan *et al.* [CMS Collaboration], Phys. Rev. Lett. **106** (2011) 212301 [arXiv:1102.5435 [nucl-ex]]; and arXiv:1410.4825 [nucl-ex].
- [4] G. Aad *et al.* [ATLAS Collaboration], Phys. Rev. Lett. **110** (2013) 022301 [arXiv:1210.6486 [hep-ex]].
- [5] S. Chatrchyan *et al.* [CMS Collaboration], Phys. Rev. Lett. **113** (2014) 132301 [arXiv:1312.4198 [nucl-ex]].
- [6] D. d’Enterria, C. Loizides, in preparation.

- [7] N. Armesto *et al.*, arXiv:1407.7649 [nucl-ex].
- [8] J. Beringer *et al.* [PDG Collaboration], Phys. Rev. D **86** (2012) 010001
- [9] M. Czakon and A. Mitov, JHEP **1301** (2013) 080 [arXiv:1210.6832 [hep-ph]].
- [10] N. Kidonakis, Phys. Part. Nucl. **45** (2014) 714 [arXiv:1210.7813 [hep-ph]].
- [11] M. Czakon, P. Fiedler and A. Mitov, Phys. Rev. Lett. **110** (2013) 252004 [arXiv:1303.6254 [hep-ph]].
- [12] J. M. Campbell and R. K. Ellis, Nucl. Phys. Proc. Suppl. **205-206** (2010) 10 [arXiv:1007.3492 [hep-ph]]; <http://mcfm.fnal.gov>.
- [13] M. Czakon, M. L. Mangano, A. Mitov and J. Rojo, JHEP **1307** (2013) 167 [arXiv:1303.7215 [hep-ph]].
- [14] D. d'Enterria, in Springer Verlag Landolt-Boernstein Vol. 1-23A (2010); arXiv:0902.2011 [nucl-ex].
- [15] S. Chatrchyan *et al.* [CMS Collaboration], Phys. Rev. C **84** (2011) 024906 [arXiv:1102.1957 [nucl-ex]]; and Phys. Lett. B **712** (2012) 176 [arXiv:1202.5022 [nucl-ex]].
- [16] G. Aad *et al.* [ATLAS Collaboration], Phys. Rev. Lett. **105** (2010) 252303 [arXiv:1011.6182 [hep-ex]]; and arXiv:1411.2357 [hep-ex].
- [17] Y. L. Dokshitzer, V. A. Khoze and S. I. Troian, J. Phys. G **17**, 1602 (1991); Y. L. Dokshitzer and D. E. Kharzeev, Phys. Lett. B **519**, 199 (2001) [arXiv:hep-ph/0106202].
- [18] P. Gossiaux, J. Aichelin and T. Gousset, Prog. Theor. Phys. Suppl. **193** (2012) 110 [arXiv:1201.4038 [hep-ph]].
- [19] M. Djordjevic and M. Djordjevic, Phys. Lett. B **734** (2014) 286 [arXiv:1307.4098 [hep-ph]].
- [20] S. Alekhin, A. Djouadi and S. Moch, Phys. Lett. B **716** (2012) 214 [arXiv:1207.0980 [hep-ph]].
- [21] P. Z. Skands and D. Wicke, Eur. Phys. J. C **52** (2007) 133 [hep-ph/0703081 [hep-ph]]; S. Argyropoulos and T. Sjöstrand, JHEP **1411** (2014) 043 [arXiv:1407.6653 [hep-ph]].
- [22] H. Paukkunen and C. A. Salgado, Phys. Rev. Lett. **110** 21 (2013) 212301 [arXiv:1302.2001 [hep-ph]].
- [23] H. Paukkunen and P. Zurita, JHEP **1412** (2014) 100 [arXiv:1402.6623 [hep-ph]].
- [24] H.-L. Lai *et al.*, Phys. Rev. D **82** (2010) 074024 [arXiv:1007.2241 [hep-ph]].
- [25] M. Arneodo, Phys. Rept. **240** (1994) 301.
- [26] K. J. Eskola, H. Paukkunen and C. A. Salgado, JHEP **0904** (2009) 065 [arXiv:0902.4154 [hep-ph]].
- [27] M. Hirai, S. Kumano and T.-H. Nagai, Phys. Rev. C **76** (2007) 065207 [arXiv:0709.3038 [hep-ph]].
- [28] I. Schienbein *et al.*, Phys. Rev. D **80** (2009) 094004 [arXiv:0907.2357 [hep-ph]].
- [29] D. de Florian, R. Sassot, P. Zurita and M. Stratmann, Phys. Rev. D **85** (2012) 074028 [arXiv:1112.6324 [hep-ph]].
- [30] S. Chatrchyan *et al.* [CMS Collaboration], Eur. Phys. J. C **74** (2014) 7, 2951 [arXiv:1401.4433 [nucl-ex]].
- [31] H. Paukkunen, K. J. Eskola and C. Salgado, arXiv:1408.4563 [hep-ph].
- [32] A. Kusina *et al.*, PoS DIS **2014** (2014) 047 [arXiv:1408.1114 [hep-ph]].
- [33] J. M. Campbell and F. Tramontano, Nucl. Phys. B **726** (2005) 109 [hep-ph/0506289].
- [34] V. Khachatryan *et al.* [CMS Collaboration], Phys. Lett. B **695** (2011) 424 [arXiv:1010.5994 [hep-ex]].
- [35] S. Chatrchyan *et al.* [CMS Collaboration], JHEP **1107** (2011) 049 [arXiv:1105.5661 [hep-ex]].

- [36] S. Chatrchyan *et al.* [CMS Collaboration], Eur. Phys. J. C **71** (2011) 1721 [arXiv:1106.0902 [hep-ex]].
- [37] S. Chatrchyan *et al.* [CMS Collaboration], Phys. Rev. D **85** (2012) 112007 [arXiv:1203.6810 [hep-ex]].
- [38] S. Chatrchyan *et al.* [CMS Collaboration], JHEP **1211** (2012) 067 [arXiv:1208.2671 [hep-ex]].
- [39] S. Chatrchyan *et al.* [CMS Collaboration], Eur. Phys. J. C **73** (2013) 2339 [arXiv:1211.2220 [hep-ex]].
- [40] S. Chatrchyan *et al.* [CMS Collaboration], Eur. Phys. J. C **73** (2013) 2386 [arXiv:1301.5755 [hep-ex]].
- [41] S. Chatrchyan *et al.* [CMS Collaboration], JHEP **1402** (2014) 024 [Erratum-ibid. **1402** (2014) 102] [arXiv:1312.7582 [hep-ex]].
- [42] G. Aad *et al.* [ATLAS Collaboration], Eur. Phys. J. C **71** (2011) 1577 [arXiv:1012.1792 [hep-ex]].
- [43] G. Aad *et al.* [ATLAS Collaboration], Phys. Lett. B **707** (2012) 459 [arXiv:1108.3699 [hep-ex]].
- [44] G. Aad *et al.* [ATLAS Collaboration], Phys. Lett. B **711** (2012) 244 [arXiv:1201.1889 [hep-ex]].
- [45] G. Aad *et al.* [ATLAS Collaboration], JHEP **1205** (2012) 059 [arXiv:1202.4892 [hep-ex]].
- [46] V. Khachatryan *et al.* [CMS Collaboration], JHEP **1406** (2014) 090 [arXiv:1403.7366 [hep-ex]].
- [47] G. Aad *et al.* [ATLAS Collaboration], Phys. Lett. B **717** (2012) 89 [arXiv:1205.2067 [hep-ex]].
- [48] G. Aad *et al.* [ATLAS Collaboration], Eur. Phys. J. C **73** (2013) 1, 2261 [arXiv:1207.5644 [hep-ex]].
- [49] S. Chatrchyan *et al.* [CMS Collaboration], Phys. Rev. Lett. **107** (2011) 091802 [arXiv:1106.3052 [hep-ex]].
- [50] S. Chatrchyan *et al.* [CMS Collaboration], JHEP **1212** (2012) 035 [arXiv:1209.4533 [hep-ex]].
- [51] G. Aad *et al.* [ATLAS Collaboration], Phys. Lett. B **717** (2012) 330 [arXiv:1205.3130 [hep-ex]].
- [52] G. Aad *et al.* [ATLAS Collaboration], Phys. Rev. D **90** (2014) 112006 [arXiv:1406.7844 [hep-ex]].
- [53] S. Chatrchyan *et al.* [CMS Collaboration], Phys. Rev. Lett. **110** (2013) 022003 [arXiv:1209.3489 [hep-ex]].
- [54] S. Chatrchyan *et al.* [CMS Collaboration], Phys. Rev. Lett. **112** (2014) 231802 [arXiv:1401.2942 [hep-ex]].
- [55] G. Aad *et al.* [ATLAS Collaboration], Phys. Lett. B **716** (2012) 142 [arXiv:1205.5764 [hep-ex]].
- [56] V. Khachatryan *et al.* [CMS Collaboration], “Heavy Ions Projections at HL-LHC”, CMS-PAS-FTR-13-025.
- [57] M. Cacciari, G. P. Salam and G. Soyez, JHEP **0804** (2008) 063 [arXiv:0802.1189 [hep-ph]].
- [58] J. Pumplin *et al.*, Phys. Rev. D **65** (2001) 014013 [hep-ph/0101032].
- [59] W. T. Giele and S. Keller, Phys. Rev. D **58** (1998) 094023 [hep-ph/9803393].
- [60] N. Sato, J. F. Owens and H. Prosper, Phys. Rev. D **89** (2014) 114020 [arXiv:1310.1089 [hep-ph]].
- [61] S. Albino, B. A. Kniehl and G. Kramer, Nucl. Phys. B **803** (2008) 42 [arXiv:0803.2768 [hep-ph]].
- [62] S. S. Adler *et al.* [PHENIX Collaboration], Phys. Rev. Lett. **98** (2007) 172302 [nucl-ex/0610036].